Forest Chemicals Review
www.forestchemicalsreview.com
ISSN: 1520-0191
September-October 2021 Page No. 748-766
Article History: Received: 22 July 2021 Revised: 16 August 2021 Accepted: 05 September 2021 Publication: 31 October 2021

Partial Discharge Localization Method for Individual Operation Based on Double Antenna Array

Songyuan Li[1], Bowen Guo[1], Qinghua Tang[1], Nan Li[1], Penfei Li[2]*
[1]State Grid Tianjin Electric Power Company Electric Power Research Institute, Tianjin, China
[2]School of Electrical and Mechanical Engineering, Pingdingshan University, Pingdingshan 467000, China
*Corresponding Author.

Abstract:

To improve the efficiency and accuracy of partial discharge (PD) location in substation, a new method for individual operation is proposed based on ultra-high frequency (UHF) method. In specialty, two UHF sensors are used to build antenna array for measuring the azimuth of PD source, the efficiency and accuracy were improved by studying the accuracy influencing factors and weights of the PD localization model through the sensitivity analysis method. And then, the method is simplified, and the system error, influencing factors, and weight of the simplified method are analyzed. The PD location device for individual operation is developed and tested in a 500 kV substation. The result shows that the method has high accuracy for measuring the azimuth, and the error is smaller as the angle between PD source and antenna array is closer to 90°, and the accuracy can be further improved by adjusting the angle of the antenna array and improving the sampling rate. The study provides important significance for improving the accuracy and efficiency of PD localization in substation.

Keywords*: Double antenna array, PD location, Individual operation, Error analysis.*

I. INTRODUCTION

Ultra-high frequency (UHF) electromagnetic wave signal radiated by partial discharge (PD) is widely used in PD localization thanks to its stable propagation speed and strong anti-interference capability [1-2]. The substation detection efficiency could be effectively improved through the UHF method for PD localization detection, which carries important engineering significance [3-5].

The UHF method is one of the major approaches for substation PD localization. The basic strategy is that four UHF antennas are used to build an antenna array, and then the partial discharge localization based on the time difference of arrival (TDOA) method is used for substation PD localization [6-8]. There are three forms of substation PD localization equipment: the first is to place four omnidirectional

Forest Chemicals Review
www.forestchemicalsreview.com
ISSN: 1520-0191
September-October 2021 Page No. 748-766
Article History: Received: 22 July 2021 Revised: 16 August 2021 Accepted: 05 September 2021 Publication: 31 October 2021

antennas at a specific location in the substation [9] to establish a coordinate system in the detection space and perform PD source localization based on the TDOA algorithm, RSSI algorithm [10-13]; The second is to place the antenna array on the vehicle roof and drive the vehicle to perform inspection and localization in the substation [14]; the third is to install the antenna array on the top of the substation control room for PD source localization [15]. Literature [16] proposes to use two antennas to build an antenna array, and the three-dimensional PD is localized through the substation through rotational multi-orientation measurement. The above methods could complete the substation PD localization task, but limited by the heavy equipment, the special heavy-duty mobile equipment is needed to load the localization device, and multiple people are required for cooperative operation. In terms of localization error analysis, literature [17] analyzes the error of the four-antenna rectangular array; literature [9] analyzes the influencing factors in direction of arrival and the localization error of various forms of four-antenna array based on the Monte Carlo algorithm. The above analysis results show that PD source azimuth has much higher accuracy than distance. In practical applications, the two-dimensional azimuth is used as the localization result.

This work proposed a substation PD localization method for individual operation, which is able to improve the accuracy and efficiency of PD localization in the substation. First, analyze the mathematical model of PD localization based on the dual-antenna array, and use the sensitivity analysis method to analyze the parameters and weights that affect the localization accuracy; Second, in view of the analysis results, a PD localization method suitable for individual operation based on the dual-antenna array is proposed, and then the influence of the system parameters and their weights for the system error and localization are analyzed Finally, a substation PD localization device suitable for individual operation is designed, tested and verified in a 500kV substation.

II. PARTIAL DISCHARGE LOCALIZATION METHOD FOR INDIVIDUAL OPERATION

2.1 PD Localization Mathematical Model Based on Dual Antenna Array

Dual antennas are used to build an antenna array for PD localization in the substation. The mathematical model of the localization principle as shown in Fig 1. The two antennas are located at A and B on the x-axis, the distance is $2r$, and the coordinate origin o is the center of the two antennas. p represents the PD source, and the coordinates are (x, y, h). The equipment height in the substation is a fixed value, and the azimuth angle θ and the elevation angle φ of the PD source relative to the antenna array will change as the detection point changes. UHF signals detected by two antennas are acquired by using a multi-channel synchronous acquisition device, and the time delay Δt of the two signals is calculated. The positional relationship between the PD source and the antenna array can be expressed as Eq. (1), where, d_{pA} and d_{pB} are the distances between the PD source and antennas A, B, respectively. c stands for the propagation speed of electromagnetic waves in the air, and the three unknowns h, φ and θ

Forest Chemicals Review
www.forestchemicalsreview.com
ISSN: 1520-0191
September-October 2021 Page No. 748-766
Article History: Received: 22 July 2021 Revised: 16 August 2021 Accepted: 05 September 2021 Publication: 31 October 2021

determine the location of the PD source. And then three sets of equations shown in Eq. (1) need to be established for simultaneous solutions for the PD source localization.

$$\begin{aligned}\Delta t &= \frac{1}{c}(\mathrm{d}_{p\mathrm{A}} - \mathrm{d}_{p\mathrm{B}}) = \frac{1}{c}\left(\sqrt{(x+r)^2 + y^2 + h^2} - \sqrt{(x-r)^2 + y^2 + h^2}\right) \\ &= \frac{1}{c}\left(\sqrt{h^2\left(1+\frac{1}{\tan^2\varphi}\right) + r^2 + \frac{2hr\cos\theta}{\tan\varphi}} - \sqrt{h^2\left(1+\frac{1}{\tan^2\varphi}\right) + r^2 - \frac{2hr\cos\theta}{\tan\varphi}}\right)\end{aligned} \tag{1}$$

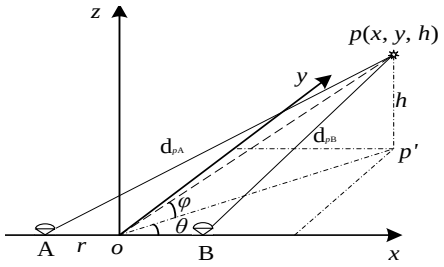

Fig 1: the model of PD localization based on double antenna array

2.1.1 Principle of sensitivity analysis

Sensitivity analysis is a method to study the sensitivity of the system state to changes in system parameters. Assume that $T(s)$ represents a linear, time-invariant system, and x is a parameter of a certain part of the system. To study the influence of small changes in x on the system, the system transfer function is expressed as $T(s, x)$. Assume that x changes slightly near the standard value x_0, the variation is $\Delta x = x - x_0$. The expanded of $T(s, x)$ at x_0 using Taylor series can be shown as Eq. (2). If the transfer function $T(s, x)$ is continuous at x_0, ignore the second and higher order terms of Δx, and then $T(s, x)$ can be expressed as Eq. (3).

$$T(s,x) = T(s,x_0) + \frac{\partial T(s,x)}{\partial x}\Big|_{x=x_0}\Delta x + \ldots + \frac{\partial^n T(s,x)}{n!\cdot\partial^n x}\Big|_{x=x_0}\Delta x^n + \ldots + R_n[T(s,x)] \tag{2}$$

$$T(s,x) = T(s,x_0) + \frac{\partial T(s,x)}{\partial x}\Big|_{x=x_0}\Delta x \tag{3}$$

The change ΔT of the system transfer function due to a slight change in parameter x is expressed as Eq. (4). Define the unnormalized sensitivity of the transfer function $T(s, x)$ relative to the system parameter x as shown as Eq. (5). The unnormalized sensitivity is the absolute change of the system

Forest Chemicals Review
www.forestchemicalsreview.com
ISSN: 1520-0191
September-October 2021 Page No. 748-766
Article History: Received: 22 July 2021 Revised: 16 August 2021 Accepted: 05 September 2021 Publication: 31 October 2021

transfer function due to the tiny change of the parameter *x*. To compare the degree of influence of different parameters on the system transfer function, it is necessary to calculate the degree of absolute change caused by each parameter relative to the transfer function of the original system, that is, the normalized sensitivity, and then shown as Eq. (6).

$$\Delta T = T(s,x) - T(s,x_0) = \frac{\partial T(s,x)}{\partial x}\Big|_{x=x_0} \Delta x \tag{4}$$

$$S_x^T = \frac{\partial T}{\partial x} \tag{5}$$

$$S_x^T = \frac{\partial T}{\partial x} \cdot \frac{x}{T} = \frac{\frac{\partial T}{T}}{\frac{\partial x}{x}} = \frac{\partial \ln T}{\partial \ln x} \tag{6}$$

The normalized sensitivity is the limit value of the ratio of the relative change in the transfer function $T(s, x)$ caused by a small change in x to the relative change in x when Δx infinitely tends to zero. $T(s)$ can be expressed as Eq. (7), where, $R(s)$, $E(s)$ are the functions of the output and input variables of the system, respectively. The partial derivative of the system transfer function $T(s)$ with respect to the parameter x is shown in Eq. (8). The normalized sensitivity of $T(s)$ to the parameter x can be shown as Eq. (9).

$$T(s) = \frac{R(s)}{E(s)} \tag{7}$$

$$\frac{\partial T(s)}{\partial x} = \frac{\partial}{\partial x}\left[\frac{R(s)}{E(s)}\right] = \frac{1}{E(s)} \cdot \frac{\partial R(s)}{\partial x} \tag{8}$$

$$S_x^{T(s)} = \frac{\partial T(s)}{\partial x} \cdot \frac{x}{T} = \frac{\partial}{\partial x}\left[\frac{R(s)}{E(s)}\right] \cdot \frac{xE(s)}{R(s)} = \frac{\partial R(s)}{\partial x} \cdot \frac{x}{R(s)} = S_x^{R(s)} \tag{9}$$

Eq. (8) and (9) show that the partial derivative of the system output with respect to x is equal to the product of the partial derivative of the transfer function with regard to x and the input variable, and the sensitivity of the system output variable to x is equal to the sensitivity of the transfer function to x. The normalized sensitivity is the ratio of the rate of change of x to the rate of change of the system output

Forest Chemicals Review
www.forestchemicalsreview.com
ISSN: 1520-0191
September-October 2021 Page No. 748-766
Article History: Received: 22 July 2021 Revised: 16 August 2021 Accepted: 05 September 2021 Publication: 31 October 2021

$R(s)$, and expressed as Eq. (10), where, $dR(s)/R(s)$ is the rate of change of the output variable, dx/x is the rate of change of parameter x.

$$\frac{dR(s)}{R(s)} = S_x^{T(s)} \cdot \frac{dx}{x} \tag{10}$$

2.1.2 Factors influencing localization accuracy and weight analysis

According to the analysis of existing localization methods, the delay accuracy determines the localization accuracy of the PD source [16-17]. From Eq. (1), it can be known that the delay Δt is determined by the four parameters r, h, φ and θ. Where, r is the size of the antenna array and h is the height of the PD source. The two parameters are not affected by the position change in the detection process, while φ and θ are greatly affected by the inspection position.

The relationship between time delay Δt and φ, θ in the range of 0-90°as h=7.5m and r=1m is illustrated in Fig 2. When φ and θ are both 0°, Δt is the maximum value of 6.667ns, that is, the PD source is located on the extension line of the antenna array, d_{pA}-d_{pB}≈2m. When φ=90° or θ=90°, Δt is 0ns. φ=90° indicates that the PD source is located at infinity on the top of the antenna array, d_{pA}≈d_{pB}. θ=90° indicates that the projection of the PD source is located on the perpendicular bisector of the antenna array, d_{pA}=d_{pB}.

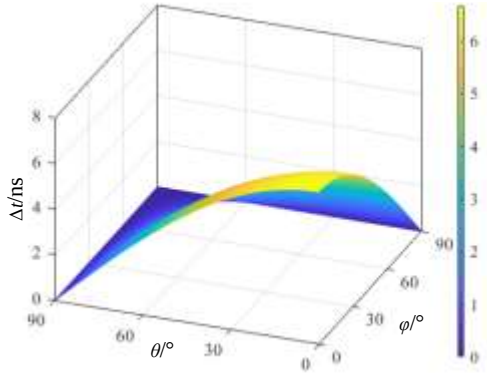

Fig 2: relationship between Δt and φ, θ when h=7.5m and r=1m

According to analysis in Section 1.1.1, take Δt as the system output and φ and θ as the system parameters, calculate the normalized sensitivity of φ and θ to Δt according to Eq. (9), and the normalized sensitivity of θ to Δt is shown as Eq. (11). When θ changes slightly, the variation of Δt can be shown as Eq. (12). In the same way, when φ changes slightly, the variation of Δt can be shown as Eq. (13). The

Forest Chemicals Review
www.forestchemicalsreview.com
ISSN: 1520-0191
September-October 2021 Page No. 748-766
Article History: Received: 22 July 2021 Revised: 16 August 2021 Accepted: 05 September 2021 Publication: 31 October 2021

deviation value of Δt when both θ and φ have a deviation of 1° in the range of 0-90° are illustrated in Fig. 3 (a) and (b).

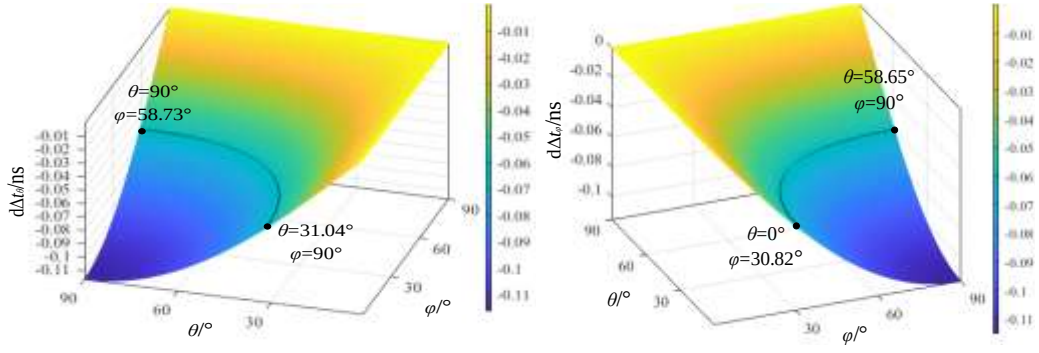

(a) The relationship between Δt and φ, θ when dθ=1° (b) The relationship between Δt and φ, θ when dθ=1°

Fig 3: the deviation of Δt when $d\theta$=1° and $d\varphi$=1°

It can be seen from Fig 3. that the maximum deviation of Δt is 0.12ns in the two deviation cases, but the deviation distribution is different. The area where the deviation of Δt caused by θ is relatively large is concentrated at θ=90°, φ=0°. That is, the PD source is located on the extension of the vertical line of the antenna array. In this area, Δt is more sensitive to the change of θ. The area with large deviation caused by φ is concentrated at θ=0°, φ=90°. That is, the PD source is located on the extension line of the antenna array and on the vertical line of the top of the antenna array. In this area, Δt is more sensitive to the change of φ. In field detection, the PD source is definitely higher than the antenna array, and the farther the detection point is from the PD source, the smaller the value of φ. Under different voltage levels of the substation, the safety distance and equipment height are also different. Take an open circuit breaker as an example. The height of 110kV equipment is about 2.5m with a safety distance of 1.5m, the height of 220kV equipment is about 7.5m with a safety distance of 3m, the height of 500kV equipment is about 12m with a safety distance of 5m. When the safety distance is guaranteed, the limit angles of φ are 59°, 68°, 67°. The black solid lines in Fig.3 (a) and (b) are contour lines with $d\Delta t$=0.06ns, and the coordinates of the starting point of the contour lines have been marked in the figure. In the range of φ<59°, $|d\Delta t_\theta|>|d\Delta t\varphi|$, θ has *a* high sensitivity to Δt. That is, a small deviation of θ leads to a larger deviation of Δt. It shows that in the localization model based on dual antennas, the azimuth angle θ calculated by using the time delay Δt of the two UHF signals has higher accuracy.

$$S_\theta^{\Delta t} = -\frac{1}{c}\left(\frac{r\sin\theta}{\tan\varphi\sqrt{\frac{1}{\tan^2\varphi}-\frac{2r\cos\theta}{h\tan\varphi}+\frac{r^2}{h^2}+1}}+\frac{r\sin\theta}{\tan\varphi\sqrt{\frac{1}{\tan^2\varphi}+\frac{2r\cos\theta}{h\tan\varphi}+\frac{r^2}{h^2}+1}}\right) \quad (11)$$

Forest Chemicals Review
www.forestchemicalsreview.com
ISSN: 1520-0191
September-October 2021 Page No. 748-766
Article History: Received: 22 July 2021 Revised: 16 August 2021 Accepted: 05 September 2021 Publication: 31 October 2021

$$d\Delta t_{\theta} = \Delta t \cdot S_{\theta}^{\Delta T} \cdot \frac{d\theta}{\theta} \tag{12}$$

$$d\Delta t_{\varphi} = \Delta t \cdot S_{\varphi}^{\Delta T} \cdot \frac{d\varphi}{\varphi} \tag{13}$$

2.2 PD Source Localization Method Based on Dual Antenna Array

2.2.1 Localization method

In summary, the PD localization method based on the dual-antenna array can estimation a more accurate azimuth angle. The method can be further simplified, and the localization principle is shown in Fig. 4. AB is the antenna at both ends of the antenna array, the distance is *2r*, *p* stand for the discharge source, *p*A and *p*B are the electromagnetic wave propagation paths. Where, △*p*BB' is an isosceles triangle, and the delay in signal reception of the two antennas A and B subject to $c*\Delta t=d_{AB}$. When the PD source is far away from the antenna array, the propagation paths *p*A and *p*B of the UHF signal can be approximated as parallel lines, denote as: *p*'A//*p*"B. In the figure, B" is the foot of point B on the straight line *p*'A. The path distance difference $c*\Delta t$=AB' can be approximated as $c*\Delta t\approx$AB". Then the apparent azimuth angle θ_{app} can be calculated by Eq. (14).

$$\theta_{app} = \arccos\frac{c \cdot \Delta t}{2r} \tag{14}$$

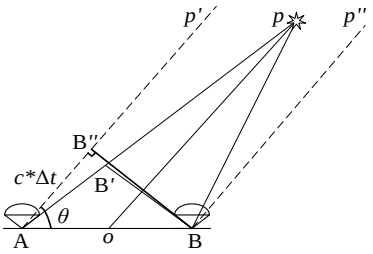

Fig 4: azimuth location method of PD source based double antenna array

2.2.2 Analysis of error

The calculation method of PD-source azimuth angle derived from Eq. (14) has two premise assumptions: (1) the PD source and the antenna array are in the same plane; (2) the distance between the PD source and the antenna array $op \gg 2r$. Therefore, it will inevitably lead to a certain error between θ_{app}

Forest Chemicals Review
www.forestchemicalsreview.com
ISSN: 1520-0191
September-October 2021 Page No. 748-766
Article History: Received: 22 July 2021 Revised: 16 August 2021 Accepted: 05 September 2021 Publication: 31 October 2021

calculated by Eq. (14) and θ in Fig.1, which is unavoidable in engineering applications. The error can be expressed as Eq. (15). The distribution relationship of $\Delta\theta$ with φ and θ when r=1m and h=7.5m is shown in Fig. 5(a). The minimum value of $\Delta\theta$ is 0°, which appears at θ=90° and φ=0°. The maximum value of $\Delta\theta$ is 90°, which appears at θ=0° and φ=90°. The black solid line in the figure lists the contour line when $\Delta\theta$=1°, indicating that the range of small deviation of θ_{app} varies with θ and φ. The error distribution of the distance L between the detection point converted from pitch angle φ and the PD source when h=2.5m, 7.5m, 12.5m, and $\Delta\theta$=1° are illustrated in Fig. 5(b). It can be seen that when the detection point is farther from the PD source, the derived azimuth angle has higher accuracy in a larger range. The three points U, V, and W are the detection ranges corresponding to $\Delta\theta$=1° under corresponding PD source conditions of the three heights when the detection distance is 20m. The detection ranges of the three heights are: (23°-90°), (75°-90°), (84°-90°), respectively.

$$\Delta\theta=\theta_{app}-\theta=\arccos\frac{c\cdot\Delta t}{2r}-\theta \tag{15}$$

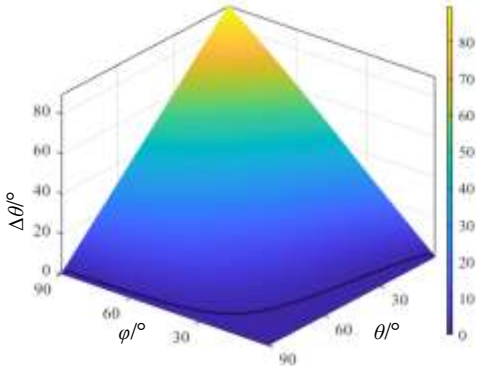

(a) The relationship between $\Delta\theta$ and φ, θ (r=1m, h=7.5m)

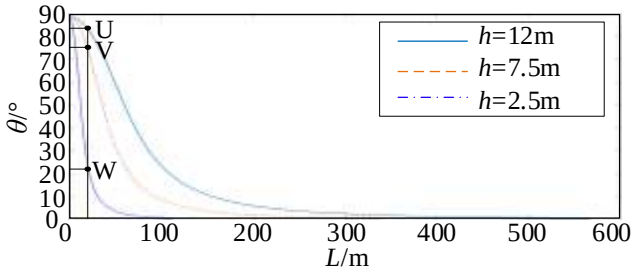

(b) distribution of $\Delta\theta$ at different heights

Fig 5: azimuth deviation with the distribution of $\Delta\theta$

Forest Chemicals Review
www.forestchemicalsreview.com
ISSN: 1520-0191
September-October 2021 Page No. 748-766
Article History: Received: 22 July 2021 Revised: 16 August 2021 Accepted: 05 September 2021 Publication: 31 October 2021

2.2.3 Analysis of the influence on localization accuracy

In Eq. (14), the parameters r and Δt have a greater impact on θ_{app} accuracy. In patrol and localization of partial discharge in the substation, the size of the antenna array is restricted due to the safety distance requirement. The research in this paper limits the range to r=0.6~1.2m. Δt is the product of the number of sampling points and the sampling interval, and the resolution is the sampling interval. Therefore, θ_{app} is also discontinuous which is calculated by Eq. 14. The distributions of θ_{app} with r and Δt are shown in Fig. 6. On the straight line from (Δt, r) = (4, 0.6) to (Δt, r) = (8, 1.2), θ_{app} is 0°. In the actual installation process, it is unavoidable that there will be a certain deviation in r, and this deviation will have an impact on the localization accuracy. There are also errors in the time delay Δt, which derive from two aspects: (1) the random error caused by the time delay estimation algorithm, and (2) the system error caused by the sampling rate of the sampling device. Random errors can be reduced or even eliminated by improving the time delay estimation algorithm. System errors are caused by sampling interval errors and are unavoidable. To analyze the influence of tiny errors of r and Δt on the localization results under different antenna array sizes and different time delays, the sensitivity analysis of Eq. 14 is performed. The sensitivity of θ_{app} to Δt can be calculated as Eq. (16). And the sensitivity of θ_{app} to r is given by Eq. (17). Assume that the sampling rate is 10GS/s, then the delay resolution is 100ps, and the minimum theoretical error is 50ps. When an error of 50ps occurs in the time delay, the deviation distribution of θ_{app} is shown in Fig 7(a). Within the same range, when the antenna array has a deviation of 1 cm, the θ_{app} deviation distribution is shown in Fig 7(b).

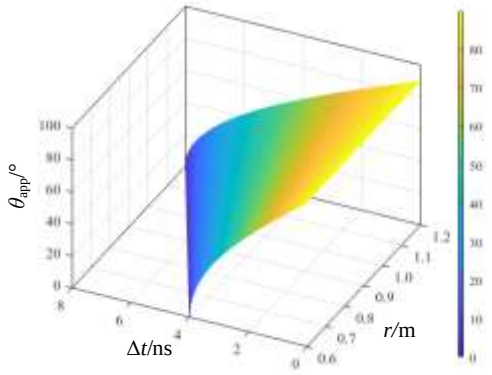

Fig 6: relationship between θ_{app} and r, Δt

Forest Chemicals Review
www.forestchemicalsreview.com
ISSN: 1520-0191
September-October 2021 Page No. 748-766
Article History: Received: 22 July 2021 Revised: 16 August 2021 Accepted: 05 September 2021 Publication: 31 October 2021

$$d\theta_{\text{app}}\big|_{\Delta t} = -\frac{90c}{\pi r\sqrt{1-\frac{c^2t^2}{4r^2}}}\cdot d\Delta t \tag{16}$$

$$d\theta_{\text{app}}\big|_{r} = -\frac{90c\cdot\Delta t}{\pi r^2\sqrt{1-\frac{c^2t^2}{4r^2}}}\cdot dr \tag{17}$$

The black solid line in Fig. 7(a) is the contour line with $|d\theta_{app}|$=1°. The starting and ending points of this contour line are (Δt, r) = (2.78, 0.6), (Δt, r) = (7.48, 1.2) respectively. There shows that in the range of Δt>2.78ns and r>0.6m, the time delay estimate has a deviation of 50ps, resulting in an error of less than 1° in θ_{app}. This range corresponds to the θ_{app} range in Fig.6 as shown in Fig.7(c). The smallest angle range is 44° to 90° when r=0.6m, which means that as θ_{app} is greater than 44°, the azimuth error due to time delay system error is less than 1°. The black solid line in Fig.7(b) is the contour line with $|d\theta_{app}|$=1°, and the starting and ending points of the contour line are (Δt, r) = (2.9, 0.6), (Δt, r) = (7.23, 1.2)), indicating that within the range of Δt>2.9ns and r>0.6, when the size of the antenna array has a deviation of 2cm, the azimuth error is less than 1°. This range corresponds to the θ_{app} range in Fig.6 as shown in Fig.7(d). The smallest angular range is 43.04° to 90° when r=0.6m, which means that when the detected apparent azimuth angle is greater than 43.04°, the localization error caused by the antenna array installation error of 2cm is less than 1°.

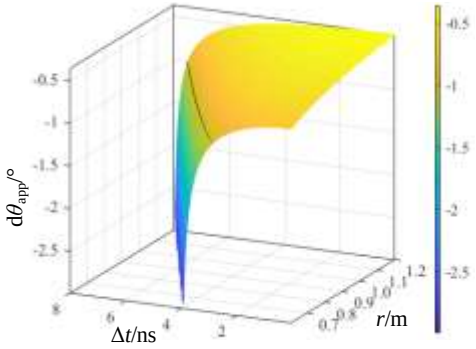

(a) the relationship between the $d\theta_{app}$ and r, Δt ($d\Delta t$=50ps)

Forest Chemicals Review
www.forestchemicalsreview.com
ISSN: 1520-0191
September-October 2021 Page No. 748-766
Article History: Received: 22 July 2021 Revised: 16 August 2021 Accepted: 05 September 2021 Publication: 31 October 2021

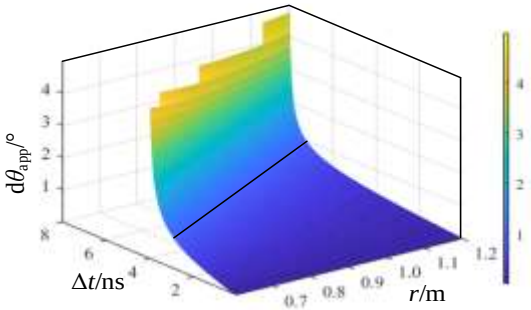

(b) the relationship between the dθ_{app} and r, Δt (dr=1cm)

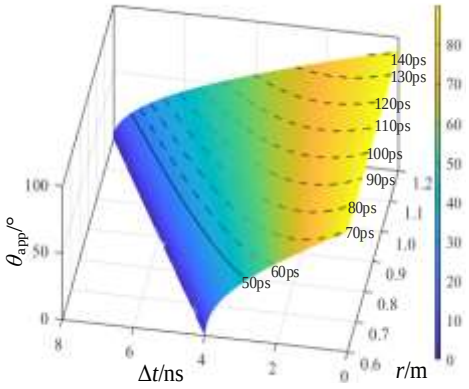

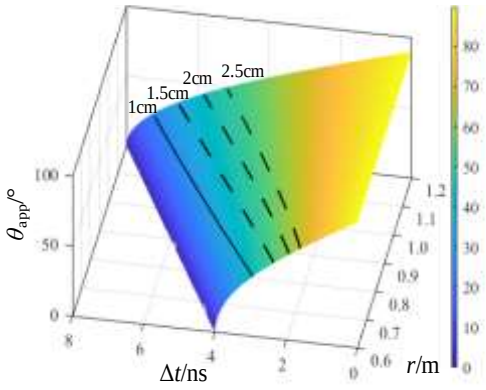

(c) the relationship between θ_{app} and r, Δt with different dΔt

(d) the relationship between θ_{app} and r, Δt with different antenna array size deviations

Fig 7: relationship between θ_{app} and r, Δt with different errors

In Fig 7(c), the black dashed line is used to list from bottom to top the range of θ_{app} corresponding to different antenna array sizes when $d\Delta t$=60ps, 70ps, 80ps, 90ps, 100ps, 110ps, 120ps and dθ_{app} =1°. It can be seen that as the time delay error increases, the angular range corresponding to the same θ_{app} detection accuracy gradually decreases. To acquire more accurate detection results, there have two approaches: (1) increase the size of the antenna array; (2) reduce the detection range, that is, adjust the detection angle to

Forest Chemicals Review
www.forestchemicalsreview.com
ISSN: 1520-0191
September-October 2021 Page No. 748-766
Article History: Received: 22 July 2021 Revised: 16 August 2021 Accepted: 05 September 2021 Publication: 31 October 2021

locate the PD source on the perpendicular bisector of the two antennas.

In Fig 7(d), the black dashed line is used to list from bottom to top the range of θ_{app} corresponding to different antenna array sizes when dr=1.5cm, 2.0cm, 2.5cm, and $d\theta_{app}$ =1°. It can be seen that as the deviation in the antenna array size increases, the detection range corresponding to the same θ_{app} accuracy gradually decreases. However, even when dr=2.5cm, the installation distance of the corresponding antenna array deviates by 5cm from the theoretical distance. At this time, when r=0.6m, the detection range corresponding to $d\theta_{app}$=1° is still (63.45°~90°). In the analysis result of Fig.7(c), when $d\Delta t$=120ps, the detection range is reduced to (89.2°~90°) even if r=1.2m and $d\theta_{app}$ =1°. Under sampling rate 10GS/s and sampling interval 100ps, the final localization error definitely exceeds 1° when a deviation between the two sampling points occurs in the time delay estimation result. In summary, the weight of the influence of Δt on the localization accuracy is much greater than the size deviation of the antenna array. There are two approaches to improve localization accuracy. One is to adjust the angle of the antenna array, and then adjust the PD source to the vertical position of the antenna array; the other is to increase the sampling frequency of the signal, and reasonably design the size of the antenna array according to the sampling rate.

III DESIGN AND TEST OF LOCALIZATION DEVICE FOR INDIVIDUAL OPERATION

3.1 Software and Hardware Design of the Localization Device

The overall architecture of the PD localization device for individual operation is shown in Fig 8. The device includes a backpack detection part and a handheld analysis terminal part. The backpack detection part includes an antenna array, a signal conditioning circuit, and a signal acquisition module. The improved Vivaldi antenna [18-19], is adopted which is a directional antenna that has the size of 258mm×150mm×0.8mm, working bandwidth is 0.5-3GHz, and the maximum gain is 7.9dBi. The signal conditioning circuit adopts a radio frequency amplifier module with a gain of 30dB. The Pico6404E virtual oscilloscope is used as the signal acquisition device with a sampling rate of 5GS/s, an analog bandwidth of 1G, a vertical resolution of 12bit, and a trigger working mode. The virtual oscilloscope weights 1.6kg, which is suitable for individual operation. The signal conditioning circuit and signal acquisition module are installed in the detection host, and a double-shoulder strap suitable for individual operation is designed to adapt to the carrying inspection in the substation. The handheld analysis terminal adopts an industrial control tablet computer, which uses a USB interface to communicate with the backpack detection device. The configuration of the tablet computer is as follows: CPU model i5-7200, memory 8GS/s, and basic frequency 3.6GHz. When time delay estimation is performed on the handheld analysis terminal, the time delay estimation algorithm adopts the minimum energy accumulation algorithm [20], and performs statistical analysis and result display of the apparent azimuth angle. According to the analysis in section 1.2.3, in order to improve the localization accuracy,

Forest Chemicals Review
www.forestchemicalsreview.com
ISSN: 1520-0191
September-October 2021 Page No. 748-766
Article History: Received: 22 July 2021 Revised: 16 August 2021 Accepted: 05 September 2021 Publication: 31 October 2021

optimization design should be performed from two aspects: increasing the signal sampling rate and the size of the antenna array. According to the argumentation results of the existing research [20], the interpolation algorithm can effectively improve the accuracy of time delay estimation. When the interpolation point is 3, the sampling rate of 5GS/s is increased to 20G, and the theoretical error at this time is reduced to 25ps. The $d\Delta t$=50ps corresponding to the solid line in Fig 7(c) already meets a sampling point delay deviation. Take r=1m, that is, the distance between the two antennas is 2m. According to the above design, the partial discharge localization device for individual operation is shown in Fig 9(a). LabView is used to develop handheld terminal detection and localization software, as shown in Fig 9(b).

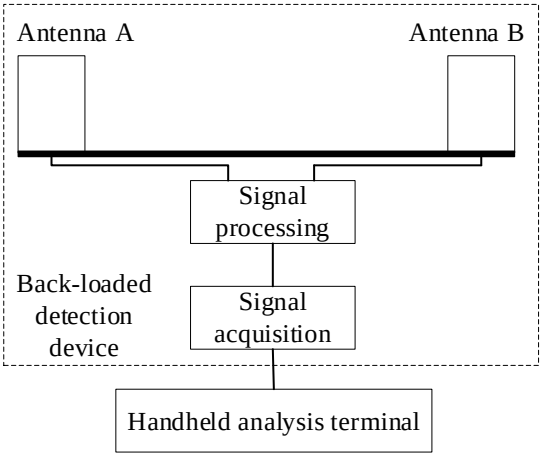

Fig 8: diagram of PD localization device for individual operation

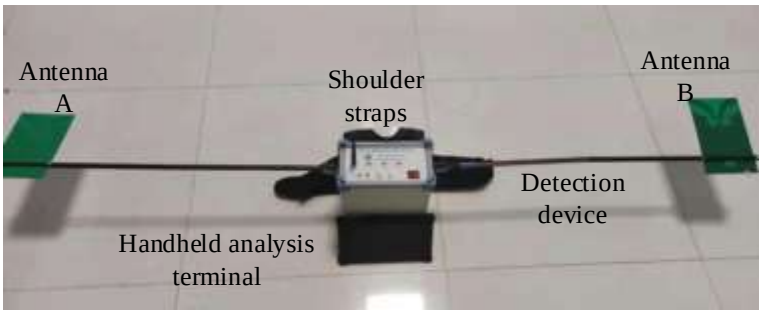

(a) partial discharge localization device hardware for individual operation

Forest Chemicals Review
www.forestchemicalsreview.com
ISSN: 1520-0191
September-October 2021 Page No. 748-766
Article History: Received: 22 July 2021 Revised: 16 August 2021 Accepted: 05 September 2021 Publication: 31 October 2021

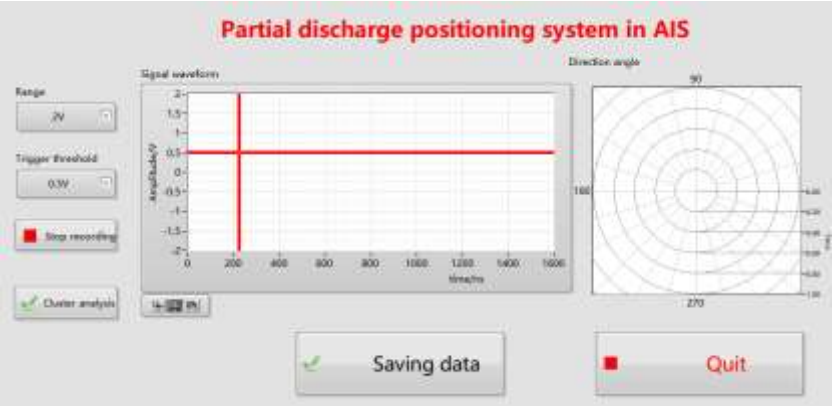

(b) upper computer software interface

Fig 9: PD localization device for individual operation

3.2 On-Site Experimentation in Substation

3.2.1 On-site experimentation

The proposed PD localization method was verified in this section using on-site experimentation at a 500kV subsection, as shown in Fig. 10(a). The online monitoring equipment installed in the area is shown in Fig. 10(a), and the UHF signal PRPS pattern is shown in Fig. 10(b). According to the pattern analysis, it can be seen that the discharge type is floating potential discharge, and the discharge intensity is -34.4dBm, but the specific discharge equipment is unclear. The PD localization device proposed in this paper is used to detect this area. Four different antenna array directions are set for detection, and the resulting apparent azimuths are shown in Figure 11(a), with a total of 4 clusters of apparent azimuths. From left to right, the average values of the four clusters of azimuth are 69.53°, 78.96°, 89.64°, and 105.74°, respectively. Fig. 11(b) lists one group of the detected original time-domain signals. The sampling rate of this signal is 5GS/s. The signal after three times interpolation is shown in Fig. 11(c), and the equivalent sampling rate reaches 20GS/s. According to the analysis of the localization method in Section 1.2, the delays of the two signals before and after the interpolation are 2ns and 2.35ns, respectively. The corresponding apparent azimuth angles are 72.54° and 69.36°, respectively.

Forest Chemicals Review
www.forestchemicalsreview.com
ISSN: 1520-0191
September-October 2021 Page No. 748-766
Article History: Received: 22 July 2021 Revised: 16 August 2021 Accepted: 05 September 2021 Publication: 31 October 2021

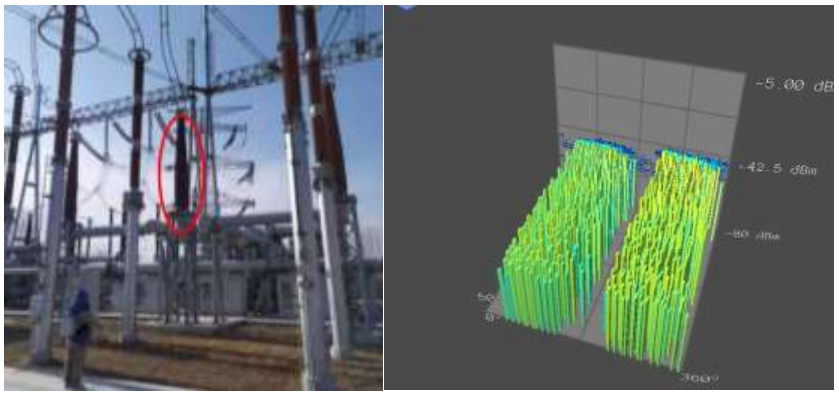

(a) inspection site (b) online monitoring results

Fig 10: substation testing site

The average azimuth and standard deviation of the four clusters of signals are illustrated in Fig. 11(d). It can be seen that at each detection angle, the deviation of θ_{app} obtained before interpolation is greater than that after interpolation, indicating that the random error can be eliminated to a certain extent after interpolation. At the same time, the closer the apparent azimuth angle is to 90°, the smaller the deviation in the obtained apparent azimuth angle before and after interpolation, which indicates that the system error is the smallest in the 90° direction, and the sampling rate has the smallest influence on the localization result. This is consistent with the analysis conclusions in Sections 1.3.2 and 1.3.3. After cross localization at multiple azimuth angles, lock the casing surrounded by the red ellipse in Fig. 10(a), and then the detection point is about 23 meters away from the device.

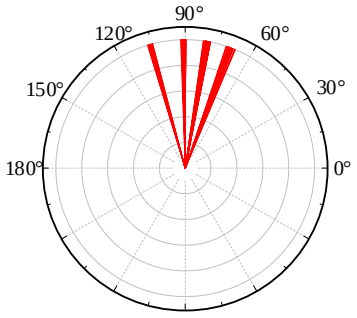

(a) the apparent azimuth angles detected in different antenna array directions

Forest Chemicals Review
www.forestchemicalsreview.com
ISSN: 1520-0191
September-October 2021 Page No. 748-766
Article History: Received: 22 July 2021 Revised: 16 August 2021 Accepted: 05 September 2021 Publication: 31 October 2021

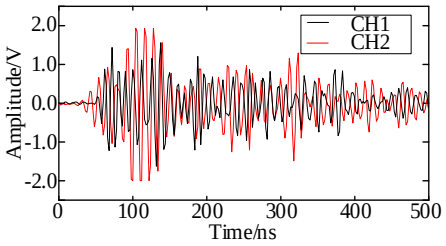

(b) the two UHF signals before interpolation

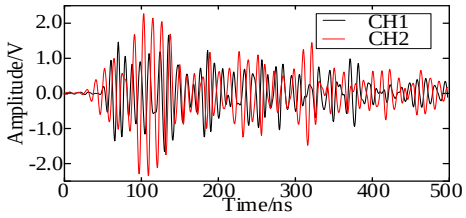

(c) the two UHF signals after interpolation

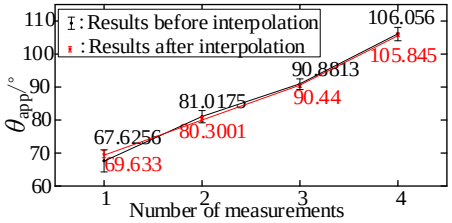

(d) analysis of root mean square error of azimuth angle before and after interpolation

Fig 11: field test results

3.2.2 Disassembly inspection

Disassembly inspection was performed on the device. The disassembly position is the flange between the two raised seats at the lower part of the casing. The position of the drawing and the casing is shown in the red mark in Fig 12. After removing the end cover at the lower part of the shielding case in the casing, it was found that there was a large amount of black powder generated by the discharge at the bonding part of the end cover and the upper shielding case, as shown in Fig 13. After removing the end cover of the shielding cover, it was found that there were two discharge traces at the position corresponding to the fastening bolt at the connection with the support insulator. At the same time, there were discharge traces on the surface of the fastening bolt and the gasket, and there was no metallic luster, as shown in Fig 14. Using a torque wrench, it was found that 5 of the 8 M12X30 hexagon socket screws connecting the middle shielding cylinder and the 4 insulating supports in the casing were loose.

Forest Chemicals Review
www.forestchemicalsreview.com
ISSN: 1520-0191
September-October 2021 Page No. 748-766
Article History: Received: 22 July 2021 Revised: 16 August 2021 Accepted: 05 September 2021 Publication: 31 October 2021

Fig 12: location of disassembly

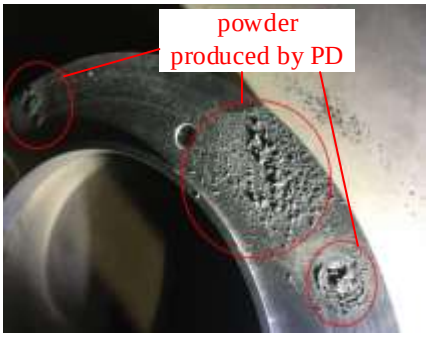

Fig 13: black powder produce by PD

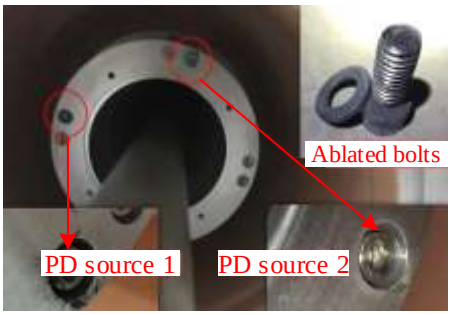

Fig 14: tighten bolts between shielding cover and supporting insulation

IV. CONCLUSION

(1) The sensitivity analysis method was used to study the sensitivity of the azimuth and elevation angles to the localization results based on the dual-antenna array PD localization mathematical model. The results show that the azimuth angle has a greater weight of influence on the time delay than the elevation angle, so more accurate azimuth can be obtained in field applications.

Forest Chemicals Review
www.forestchemicalsreview.com
ISSN: 1520-0191
September-October 2021 Page No. 748-766
Article History: Received: 22 July 2021 Revised: 16 August 2021 Accepted: 05 September 2021 Publication: 31 October 2021

(2) A simplified localization method is proposed based on a dual antenna array. The error distribution introduced by this method presents the following rules: the closer the azimuth angle of the PD source and the antenna array is to 90°, the smaller the error, and the time delay has a much larger influence weight than the antenna array size. By adjusting the angle of the antenna array to make the PD source close to 90° and improving the delay estimation accuracy, it is possible to effectively improve the localization accuracy.

(3) A PD localization system suitable for the individual operation was developed and tested in a 500kV substation to accurately locate the faulty equipment with PD, and the faulty equipment was dismantled, so the localization results were effectively verified.

ACKNOWLEDGEMENTS

This research was supported by Science and Technology Project of State Grid Tianjin Electric Power Company (KJ21-1-9).

REFERENCES

[1] Zachariades C, Shuttleworth R, Giussani R, et al. A Wideband Spiral UHF Coupler with Tuning Nodules for Partial Discharge Detection. IEEE Transactions on Power Delivery, 2019, 34(4):1300-1308.
[2] Sharifinia S, Allahbakhshi M, Ghanbari T, et al. A New Application of Rogowski Coil Sensor for Partial Discharge Localization in Power Transformers. IEEE Sensors Journal, 2021, PP (99):1-1.
[3] Zheng Q, Luo L, Song H, et al. Intelligent Learning Approach for UHF Partial Discharge Localization in Air-insulated Substations. High Voltage, 2020, 5(1).
[4] Ning S, He Y, Yuan L, et al. A Novel Localization Method of Partial Discharge Sources in Substations Based on UHF Antenna and TSVD Regularization. IEEE Sensors Journal, 2021, (99):1-1.
[5] Wang S, He Y, Yin B, et al. Partial Discharge Localization in Substations Using a Regularization Method. IEEE Transactions on Power Delivery, 2020, PP (99):1-1.
[6] Wang S, He Y, Yin B, et al. Multi-Resolution Generalized S-Transform Denoising for Precise Localization of Partial Discharge in Substations. IEEE Sensors Journal, 2020, PP (99):1-1.
[7] Hou H, Sheng G, Li S, et al. A Novel Algorithm for Separating Multiple PD Sources in a Substation Based on Spectrum Reconstruction of UHF Signals. IEEE Transactions on Power Delivery, 2015, 30(2):809-817.
[8] Dhara S, Koley C, Chakravorti S. A UHF Sensor Based Partial Discharge Monitoring System for Air Insulated Electrical Substations. IEEE Transactions on Power Delivery, 2020, PP (99):1-1.
[9] Xu Yuefeng, Ren Shuangzan, Zhu Mingxiao, et al. Local discharge signal localization based on UHF

Forest Chemicals Review
www.forestchemicalsreview.com
ISSN: 1520-0191
September-October 2021 Page No. 748-766
Article History: Received: 22 July 2021 Revised: 16 August 2021 Accepted: 05 September 2021 Publication: 31 October 2021

antenna array and analysis of influencing factors. High Voltage Apparatus, 2019,55(02):53-60

[10] Li Z, Luo L, Sheng G, et al. UHF partial discharge localisation method in substation based on dimension-reduced RSSI fingerprint. Iet Generation, Transmission & Distribution, 2018, 12(2):398-405.

[11] Zheng Q, Luo L, Song H, et al. A RSSI-AOA Based UHF Partial Discharge Localization Method Using MUSIC Algorithm[J]. IEEE Transactions on Instrumentation and Measurement, 2021, PP (99):1-1.

[12] Beura C P, Beltle M, Tenbohlen S. Positioning of UHF PD Sensors on Power Transformers Based on the Attenuation of UHF Signals. IEEE Transactions on Power Delivery, 2019, 34(4):1520-1529.

[13] LI Zhen, LUO Lingen, ZHOU Nan, et al. A Novel Partial Discharge Localization Method in Substation Based on a Wireless UHF Sensor Array. Sensors, 2017, 17(8):1909-1927.

[14] Moore P J, Portugues I E, Glover I A. Partial discharge investigation of a power transformer using wireless wideband radio-frequency measurements. IEEE Transactions on Power Delivery, 2006, 21(1):528-530.

[15] Portugues I E, Moore P J, Glover I A, et al. RF-Based Partial Discharge Early Warning System for Air-Insulated Substations. IEEE Transactions on Power Delivery, 2009, 24(1):20-29.

[16] Li Pengfei, Zhou Wenjun, Yang Shuai, et al. A Novel Method for Partial Discharge Localization in Air insulated Substations. Iet Science Measurement & Technology, 2017, 11(3):331-338.

[17] Liu Weidong, Hu Xiaofeng. Analysis on localization error of spatial discharge source based on electromagnetic radiation detection. Journal of Microwaves, 2015, 31(4): 60-65.

[18] Xavier G, Serres A, Costa E, et al. Design and Application of a Metamaterial Superstrate on a Bio-Inspired Antenna for Partial Discharge Detection through Dielectric Windows. Sensors, 2019, 19(19):4255-4282.

[19] Liu Y, Zhou W, Yang S, et al. A Novel Miniaturized Vivaldi Antenna Using Tapered Slot Edge with Resonant Cavity Structure for Ultrawideband Applications. IEEE Antennas and Wireless Propagation Letters, 2016(15):1881-1884.

[20] Tang Lin, Hu Yue, Wang Hongbin, et al. Time delay estimation of partial discharge UHF pulse signals based on interpolation cross-relation algorithm. High Voltage Engineering, 2015, 41(010): 3320-3325.